Phys. Med. Biol. **42** (1997) 1801–1819. Printed in the UK PII: S0031-9155(97)81033-0

Determination of the optical properties of semi-infinite turbid media from frequency-domain reflectance close to the source

Alwin Kienle and Michael S Patterson

Department of Medical Physics, Hamilton Regional Cancer Centre and McMaster University, 699 Concession Street, Hamilton, Ontario, L8V 5C2 Canada

Received 15 January 1997, in final form 6 May 1997

Abstract. We investigate theoretically the errors in determining the reduced scattering and absorption coefficients of semi-infinite turbid media from frequency-domain reflectance measurements made at small distances between the source and the detector(s). The errors are due to the uncertainties in the measurement of the phase, the modulation and the steady-state reflectance as well as to the diffusion approximation which is used as a theoretical model to describe light propagation in tissue. Configurations using one and two detectors are examined for the measurement of the phase and the modulation and for the measurement of the phase and the steady-state reflectance. Three solutions of the diffusion equation are investigated. We show that measurements of the phase and the steady-state reflectance at two different distances are best suited for the determination of the optical properties close to the source. For this arrangement the errors in the absorption coefficient due to typical uncertainties in the measurement are greater than those resulting from the application of the diffusion approximation at a modulation frequency of 200 MHz. A Monte Carlo approach is also examined; this avoids the errors due to the diffusion approximation.

1. Introduction

Investigation of the physiology of tissue with visible or near-infrared light for medical diagnosis normally requires the determination of its optical properties. In order to obtain the scattering and absorption coefficients of tissue, steady-state and time-resolved techniques, in both the frequency and time domain, have been used. The radiative transfer equation and its approximation, the diffusion theory, have usually been applied as the theoretical model for light propagation in tissue (Ishimaru 1978). Diffusion theory has the advantage that simple analytical formulae can be found for certain geometries. This is the case for the semi-infinite geometry investigated in this article. The main criterion for the validity of diffusion theory is that the radiance is approximately isotropic. This criterion is better fulfilled further from any light source because the detected photons have undergone more scattering interactions. The loss of photons at boundaries also introduces anisotropy in the radiance and causes diffusion theory to be less accurate in these regions.

For measurements on accessible tissue, for example the arm (Fantini *et al* 1994) or the head (Cope and Delpy 1988), the light diffusely reflected from the tissue can be measured sufficiently far away from the source that the diffusion equation is valid. However, if measurements close to the source must be made, such as in endoscopy, application of the diffusion equation is questionable. While its validity has been investigated in the time

0031-9155/97/091801+19$19.50

domain (Hielscher *et al* 1995, Kienle and Patterson 1997), to our knowledge errors in the optical properties caused by applying the diffusion equation to frequency domain measurements have not been examined. In such measurements the source intensity is modulated at rf frequencies (typically 0.1–1.0 GHz) and the phase and steady-state reflectance of the modulated diffuse reflectance are detected at some distance(s) from the source. A number of strategies have been proposed to deduce the scattering and absorption coefficients from such measurements. In principle, phase and modulation (relative to the source) at a single distance provide sufficient information, but Pogue and Patterson (1996) have shown that superior results can be achieved by measuring the phase difference and steady-state reflectance ratio between signals at two distances. Fantini *et al* (1994) described a system which uses four source–detector distances. The experimental uncertainties associated with the measurement apparatus have a greater effect on the estimates of the tissue optical properties if the distance between source and detector is decreased because the phase and the demodulation decrease, resulting in an increase in the relative error of these quantities.

In this paper we investigate theoretically the errors in the determined absorption μ_a and the reduced scattering coefficient μ_s' caused by typical uncertainties in the measurements (section 3) and from the application of the diffusion approximation (section 4) for measurements of the reflectance from a semi-infinite medium in the frequency domain close to the source. The first task is addressed by fitting a solution of the diffusion theory to results (phase and modulation data or phase and steady-state reflectance data) from the same solution to which typical experimental errors are added, and the second by fitting a solution of the diffusion equation to data obtained from Monte Carlo simulations. Optical properties typical of tissue for red or near-infrared light are used. The absorption coefficient was varied between $0.002\ \text{mm}^{-1} < \mu_a < 0.04\ \text{mm}^{-1}$ and for the reduced scattering coefficient we used $\mu_s' = 0.5\ \text{mm}^{-1}$ and $\mu_s' = 1\ \text{mm}^{-1}$. The frequency f of the intensity modulated incident light was changed between $f \approx 100$ MHz and $f \approx 1000$ MHz and the distance from the detector to the source ρ between $\rho \simeq 1$ mm and $\rho = 10$ mm and phase and steady-state reflectance data as well as phase and modulation data were considered. Configurations that measure these quantities at one distance as well as configurations that measure them at two distances are considered. In the former case the phase and the modulation are determined relative to the source and an absolute measurement of the steady-state reflectance is assumed. (For example, this can be achieved using a calibration measurement on a tissue-simulating phantom with accurately known optical properties or by characterizing the incident beam (Kienle *et al* 1996).) In the latter case the phase difference and modulation ratio or the phase difference and the steady-state reflectance ratio between two distances is calculated. Three different solutions of the diffusion equation are introduced and their performance for determination of the optical properties is investigated by fitting them to Monte Carlo simulation results.

We also discuss a solution for the reflectance in the frequency domain which is based on the use of a single Monte Carlo simulation. Using scaling principles, this simulation can be used to generate rapidly the exact (within statistical uncertainties) reflectance for any set of optical properties (Kienle and Patterson 1996). Hence it is possible to find the set of μ_a, μ_s' values which minimizes the difference between experimental data and calculated reflectance without reliance on the diffusion approximation.

2. Theory

In section 2.1 we present three solutions of the diffusion equation which have been proposed in the literature for frequency-domain reflectance $R(\omega, \rho)$. For each solution the fluence rate Φ in the scattering medium is calculated with the extrapolated-boundary condition, but the

reflectance at the physical boundary is computed in different ways: (i) using the fluence rate term; (ii) using the flux term; and (iii) using the fluence and flux terms. The second solution is included here, because it has often been used in the literature (Moulton 1990, Fantini *et al* 1994, Pogue and Patterson 1994). The first solution has been suggested by (Haskell *et al* 1994) as a simplification of the third solution which results from the calculation of the reflectance which is most correct within the diffusion approximation (Haskell *et al* 1994). It has been shown that this physically rational solution (i.e. the third solution) works the best in the time domain (Kienle and Patterson 1997). In section 2.2 we describe Monte Carlo simulations which are used in section 4 for comparison with the various solutions of the diffusion equation. In section 2.3 it is investigated if the determination of the optical properties from measurements of the phase and steady-state reflectance or of the phase and modulation at one and two distances has an unique solution.

2.1. Solutions of the diffusion equation

At least three different boundary conditions have been applied to solve the diffusion equation for photon propagation in turbid media. The zero-boundary condition, the extrapolated-boundary condition and the partial-current boundary condition were used to calculate the reflectance from a semi-infinite turbid medium in the time domain $R(\rho, t)$ (Moulton 1990, Hielscher *et al* 1995, Kienle and Patterson 1997), in the frequency domain $R(\rho, \omega)$ (Moulton 1990, Haskell *et al* 1994, Fantini *et al* 1994) and in the steady-state domain $R(\rho)$ (Farrell *et al* 1992, Bolt and ten Bosch 1994, Kienle and Patterson 1996). These quantities are linked by the Fourier transform (Arridge *et al* 1992). In the frequency-domain method the source is sinusoidally modulated ($A \exp(\mathrm{i}\omega t)$) and thus the measured signal at the detector is also sinusoidal but the oscillation is delayed in time and the modulation is reduced. The observable quantities in the frequency domain are the phase angle θ between source and the detected signal, the modulation M and the steady-state reflectance:

$$\theta = \tan^{-1} \frac{\mathrm{Im}[R(\rho, \omega)]}{\mathrm{Re}[R(\rho, \omega)]} \tag{1}$$

$$M = \sqrt{\frac{[\mathrm{Im}\, R(\rho, \omega)]^2 + [\mathrm{Re}\, R(\rho, \omega)]^2}{[R(\rho, \omega = 0)]^2}} \tag{2}$$

$$R(\rho) = R(\rho, \omega = 0) \tag{3}$$

where $\omega = 2\pi f$. Haskell *et al* (1994) showed that the zero-boundary condition solution is the least accurate and that the solutions using the partial-current boundary condition and the extrapolated-boundary condition deliver optical coefficients that differ by less than 3% when used to fit the same data sets. (The smallest source–detector distance which they applied was $\rho = 10$ mm.) Note that the zero-boundary condition states that the fluence rate is zero on the surface of the turbid medium, while the extrapolated-boundary condition states that the fluence rate goes to zero some distance beyond the actual surface. In the partial-current boundary treatment the irradiance at the boundary is set equal to the integral of the reflected radiance over solid angle 2π (Haskell *et al* 1994). The reflected radiance is caused from the photons that approach the boundary from inside and that are reflected back due to the mismatch of the refractive index inside and outside the medium.

Haskell *et al* suggested a unification of the extrapolated-boundary and the partial-current boundary solutions. They calculated Φ from the extrapolated boundary condition and used the result from the partial-current boundary condition that the reflectance is proportional to the fluence rate to compute the reflectance. Besides this solution (denoted with R_Φ) we

investigate two additional solutions. For both solutions the fluence rate is the same as above but the reflectance is calculated either from the gradient of the fluence rate (R_f) or from the integral of the radiance over the backward hemisphere ($R_{\Phi,f}$).

The extrapolated-boundary condition states that the fluence rate is zero at an artificial extrapolated boundary which is parallel to the boundary of the turbid medium. For a semi-infinite medium irradiated with a normally incident 'pencil' beam this can be achieved using a positive source term at $z = z_0 = 1/(\mu_s' + \mu_a)$ and a negative source term at $z = -z_0 - 2z_b$, where z is the direction perpendicular to the boundary pointed into the medium. (We note that for isotropic scattering we do not in fact have one source of the incident photons but a line of isotropic sources with strengths which are exponentially damped. For anisotropic scattering the situation is in general more complicated but we have found that the single point source approximation works well.) The quantity z_b equals

$$z_b = \frac{1 + R_{\text{eff}}}{1 - R_{\text{eff}}} 2D. \tag{4}$$

R_{eff} represents the fraction of photons that is internally diffusely reflected at the boundary. Haskell *et al* (1994) found that R_{eff} equals 0.493 for a refractive index n of 1.4 which is representative of measured tissue data (Bolin *et al* 1989, Tearney *et al* 1995). $D = [3(\mu_a + \mu_s')]^{-1}$ is the diffusion coefficient. For a refractive index of $n = 1.4$ we get

$$R_\Phi(\rho, \omega) = \frac{0.17}{4\pi D} \left(\frac{\exp(-kr_1)}{r_1} - \frac{\exp(-kr_2)}{r_2} \right) \exp(\mathrm{i}\omega t) \tag{5}$$

where

$$k = \sqrt{(\mu_a c + \mathrm{i}\omega)/Dc}$$
$$r_1 = \sqrt{z_0^2 + \rho^2}$$
$$r_2 = \sqrt{(z_0 + 2z_b)^2 + \rho^2}$$

c is the velocity of light in the tissue and $\mathrm{i} = \sqrt{-1}$. The constant in equation (5) is obtained by calculating the reflectance $R(\rho, \omega)$ as the integral of the radiance over the backward hemisphere (Haskell *et al* 1994)

$$R(\rho, \omega) = \int_{2\pi} \mathrm{d}\Omega \, (1 - R_{\text{fres}}(\theta)) \frac{1}{4\pi} \left(\Phi(\rho, z = 0, \omega) + 3D \frac{\partial \Phi(\rho, z = 0, \omega)}{\partial z} \cos\theta \right) \cos\theta \tag{6}$$

where $R_{\text{fres}}(\theta)$ is the Fresnel reflection coefficient for a photon with an incident angle θ relative to the normal to the boundary. To derive equation (5) the flux term in equation (6) is replaced by

$$\frac{\partial \Phi(\rho, z = 0, \omega)}{\partial z} = \frac{1}{z_b} \Phi(\rho, z = 0, \omega) \tag{7}$$

as a result of the partial-current boundary condition (Haskell *et al* 1994).

For the second solution the fluence rate in the medium is calculated as in the first solution but the reflectance is computed with Fick's law (Moulton 1990)

$$R_f(\rho, \omega) = -D \nabla \Phi(\rho, z, \omega) \cdot (-\boldsymbol{z})|_{z=0} \tag{8}$$

yielding

$$R_f(\rho, \omega) = \frac{1}{4\pi} \left[z_0 \left(k + \frac{1}{r_1} \right) \frac{\exp(-kr_1)}{r_1^2} + (z_0 + 2z_b) \left(k + \frac{1}{r_2} \right) \frac{\exp(-kr_2)}{r_2^2} \right] \exp(\mathrm{i}\omega t). \tag{9}$$

We note that Moulton (1990) derived exact and Fantini *et al* (1994) approximate analytical formulae for the phase and modulation in this case. This solution was also used by Pogue and Patterson (1994).

The third solution also employs the extrapolated-boundary condition to derive the fluence rate and, as for the first solution, the reflectance $R_{\Phi,f}$ is calculated as the integral of the radiance over the backward hemisphere (equation (6)), but we do not use the result from the partial-current boundary condition that the flux is proportional to the fluence rate as was applied for the derivation of R_Φ (equation (7)). For a refractive index $n = 1.4$ equation (6) gives (Kienle and Patterson 1997)

$$R_{\Phi,f}(\rho,\omega) = \frac{0.118}{4\pi D}\left(\frac{\exp(-kr_1)}{r_1} - \frac{\exp(-kr_2)}{r_2}\right)\exp(\mathrm{i}\omega t) + 0.306R_f(\rho,\omega). \tag{10}$$

(We note that $R_{\Phi,f}(\rho,\omega)$ and $R_\Phi(\rho,\omega)$ are calculated from the total re-emitted radiance matching the conditions of the Monte Carlo simulations, see section 2.2.) We tested the mathematical correctness of the results of equations (5), (9) and (10) by comparing them with the Fourier transforms of the time-domain reflectance $R(\rho,t)$ derived from the time-domain diffusion solution and the corresponding boundary conditions.

2.2. Monte Carlo method

In section 4 the solutions of the diffusion equation are compared with Monte Carlo simulations. The principles of Monte Carlo simulation of photon transport have been thoroughly described (Wilson and Adam 1983, Wang *et al* 1995), so that we point out only the salient features of our Monte Carlo program. In order to calculate the phase and the modulation for different frequencies, the simulations were performed in the time domain using an impulse source and the observed reflectance $R(\rho,t)$ was Fourier transformed using an FFT code (Press *et al* 1990). For the time-domain Monte Carlo simulations a 'pencil' photon beam consisting of a Dirac function in time was normally incident onto the semi-infinite turbid medium. The scattering angle was calculated with the Henyey–Greenstein (Henyey and Greenstein 1941) phase function. The anisotropy factor g was chosen to be 0.8, because variation in g between 0.8 and 1 does not influence the reflectance significantly as long as μ_s' is constant (Kienle and Patterson 1996) and because simulations are faster for smaller g values. All re-emitted photons were scored independent of the emergence angle.

The simulations were run for zero absorption and for a certain reduced scattering coefficient. From these data the reflectance curves with different absorption coefficients were calculated using Beer's law and the pathlength of the photons through the turbid medium (Graaff *et al* 1993). This approach has the advantage that only one simulation is needed to generate reflectance data for different absorption coefficients and that the statistical uncertainty of the results is not limited by histories terminated by absorption events.

Spatial resolution of 0.5 mm and temporal resolution of 2.5 ps for $t < 100$ ps and of 10 ps for 100 ps $< t <$ 2 ns were chosen for scoring the reflectance. Photons that spent more than 2 ns in the turbid medium were usually artificially absorbed to decrease the computation time. However, for small absorption coefficients and large $\mu_s'\rho$ values the reflectance at $t > 2$ ns cannot be neglected, because it still influences the results of the Fourier transform. To address this problem a solution of the diffusion equation was used to calculate the reflectance for times longer than 2 ns. We compared the reflectance from the corresponding time-domain solutions of equations (5), (9) and (10) (which are connected by the Fourier transform) with that calculated from Monte Carlo simulations and found that the corresponding time-domain solution of equation (9) (equation (5) in Kienle and

Patterson (1997)) approximates the Monte Carlo data well for long times. Figure 1 shows the normalized difference between the reflectance calculated with Monte Carlo simulations R_{MC} and the above mentioned time domain solution (equation (5) in Kienle and Patterson (1997)) for $\mu_s' = 1$ mm^{-1}, $\mu_a = 0$ mm^{-1} and $\rho = 2.75, 4.75, 9.75, 14.75$ mm.

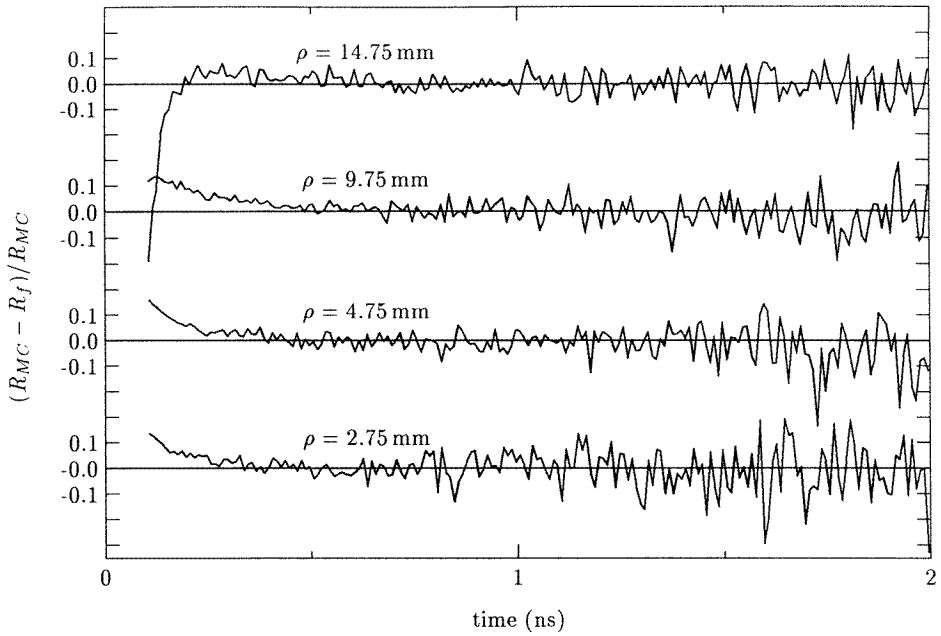

Figure 1. Comparision of time-domain reflectance obtained from Monte Carlo simulations R_{MC} and of reflectance computed with equation (5) in (Kienle and Patterson 1997) R_f. $(R_{MC} - R_f)/R_{MC}$ is shown for $\mu_s' = 1$ mm^{-1}, $\mu_a = 0$ mm^{-1} and $\rho = 2.75$, 4.75, 9.75, 14.75 mm.

From figure 1 it can be seen that this equation (equation (5) in Kienle and Patterson (1997)) approximates Monte Carlo data well for times as short as 500 ps. This is also true for non-zero absorption coefficients used in this study (figures not shown). The relative differences $(R_{MC} - R_f)/R_{MC}$ for a reduced scattering coefficient of $\mu_s' = 0.5$ mm^{-1} can also be found from figure 1 by scaling the data. In this case the number on the time axis and the distances in figure 1 must be doubled (Kienle and Patterson 1996).

The reflectance is a rapidly increasing function of time at early times and small distances ρ. The temporal resolution of the time-domain reflectance calculated with the Monte Carlo method must be high enough to ensure that no information is lost when the Fourier transform is performed. This was checked by comparing the phase and intensity values obtained by Fourier transforming a time-resolved solution of the diffusion equation (for example equation (5) in Kienle and Patterson (1997)) with the phase and intensity values from the corresponding solution in the frequency domain (equation (7)). We found that a temporal resolution of 2.5 ps produce errors which are negligible compared with typical experimental errors even for distances close to the source. Time-domain reflectance data up to 6 ns were used (2400 data points) for calculation of the Fourier transform. The remainder of the 4096-element array required for the FFT code was padded with zeros.

In section 4 solutions of the diffusion equation are fitted to Monte Carlo simulations to determine the accuracy of the diffusion approximation. For the nonlinear regression a

combination of the gradient search method and the method of linearizing the fitting function was used (Bevington 1983). Equal weights for the phase and modulation or the phase and steady-state reflectance were used in the fitting procedure.

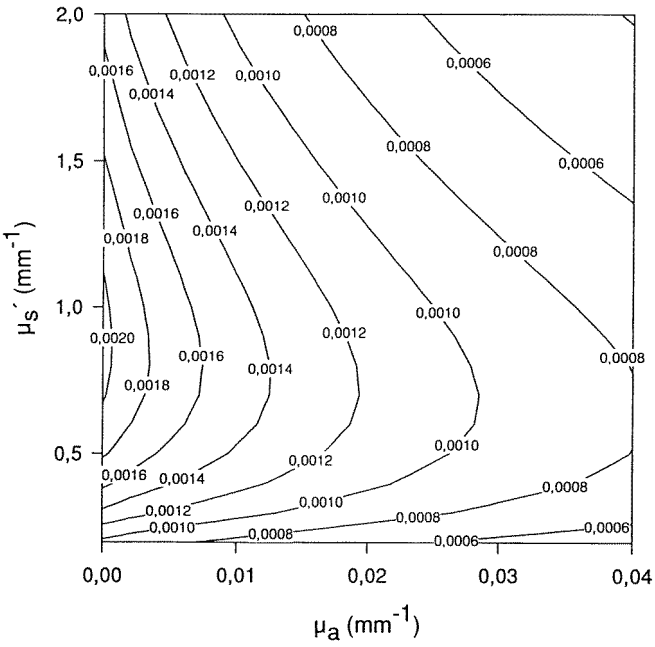

Figure 2. Contour plot of the steady-state reflectance (mm^{-2}) versus μ_a and μ_s' for $\rho = 5$ mm using equations (10) and (3).

2.3. Uniqueness of the derived optical properties

In this section it is investigated whether the phase and steady-state reflectance data or the phase and modulation data lead to a unique set of optical properties, μ_a and μ_s'. In order to examine this question we calculated these quantities with equation (10) and present them versus the optical properties in a contour plot. Figure 2 (figure 3) shows the steady-state reflectance (phase) versus the absorption and reduced scattering coefficients for a distance of 5 mm and a modulation frequency of 200 MHz. As expected, an increase in the absorption coefficient for a constant reduced scattering coefficient results in a decreased steady-state reflectance. However, if the absorption coefficient is constant and the reduced scattering coefficient is changed, two values of μ_s' exist which result in the same steady-state reflectance. Comparing figure 2 with figure 3 it can be seen that the isophase lines can intersect with the isosteady-state reflectance lines at more than one point. This means that the determination of the optical properties is not unique if phase and steady-state reflectance are measured at a single point close to the source. We note that this ambiguity is not a result of the inaccuracy of the diffusion equation. For a certain distance ρ from the source and constant μ_a there always exist a maximum of $R(\rho)$.

Figure 4 shows the contour plot for the steady-state reflectance ratio at the distances $\rho_2 = 2.5$ mm and $\rho = 5$ mm. (The smaller distance is termed ρ_2 and the larger distance ρ.) In this case only one reduced scattering coefficient exists that results in a certain value of

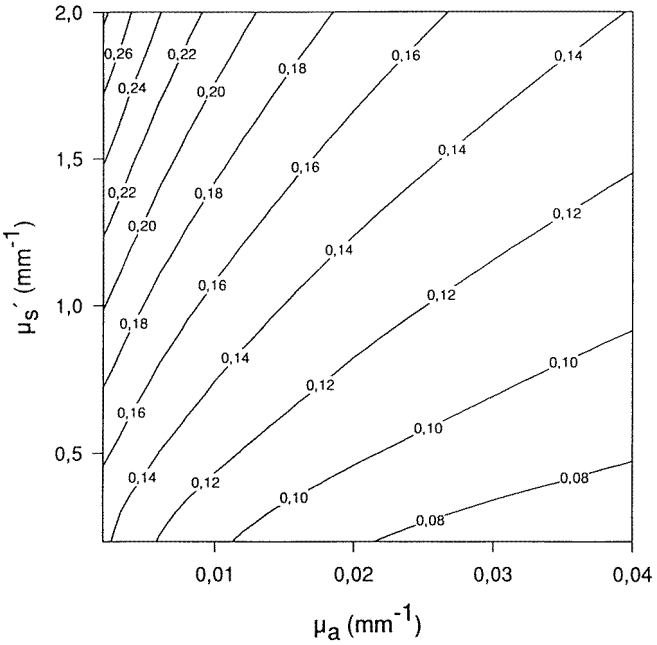

Figure 3. Contour plot of the phase (radians) versus μ_a and μ_s' for $\rho = 5$ mm using equations (10) and (1). The modulation frequency is 200 MHz.

the steady-state reflectance ratio for a constant absorption coefficient. Because the contour plot of the relative phase for these distances (figure not shown) is qualitatively similar to figure 3, it follows that measurements of the phase difference and steady-state reflectance ratio between two distances result in an unique set of absorption and reduced scattering coefficients.

For phase and modulation data similar investigations show that the determination of the optical properties is unique for data measured at one or two distances.

3. Derivation of the optical coefficients for typical mean experimental errors in the measurements

In order to investigate how experimental uncertainties in the phase, steady-state reflectance and modulation influence the determination of the optical properties, these quantities were calculated for given values of the distance, frequency, absorption and reduced scattering coefficients, using equation (10), and errors typical of a well designed apparatus were added (Pogue and Patterson 1996). A nonlinear regression also applying equation (10) was used to determine μ_a and μ_s' from these error-added-values. For the instrumental errors normal distributions having standard deviations of 0.1° for the phase and 0.001 for the modulation were sampled, and for the steady-state reflectance a relative error with a standard deviation of 0.001 was used (Pogue and Patterson 1996, Fantini *et al* 1994, Bocher *et al* 1995). For each set of parameters the nonlinear regression was performed with 200 different samples from the error distribution (Pogue and Paterson 1996) and the relative standard deviations (standard deviation divided by the correct value) of the obtained μ_a and μ_s' were calculated. In the following this quantity is termed σ_a (σ_s) when the absorption coefficient

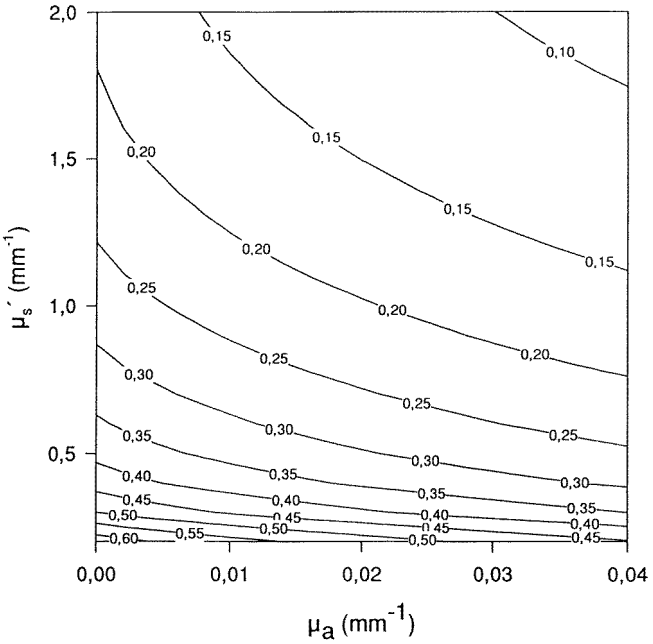

Figure 4. Contour plot of the steady-state reflectance ratio at $\rho = 5$ mm and $\rho_2 = 2.5$ mm versus μ_a and μ_s' using equations (10) and (3).

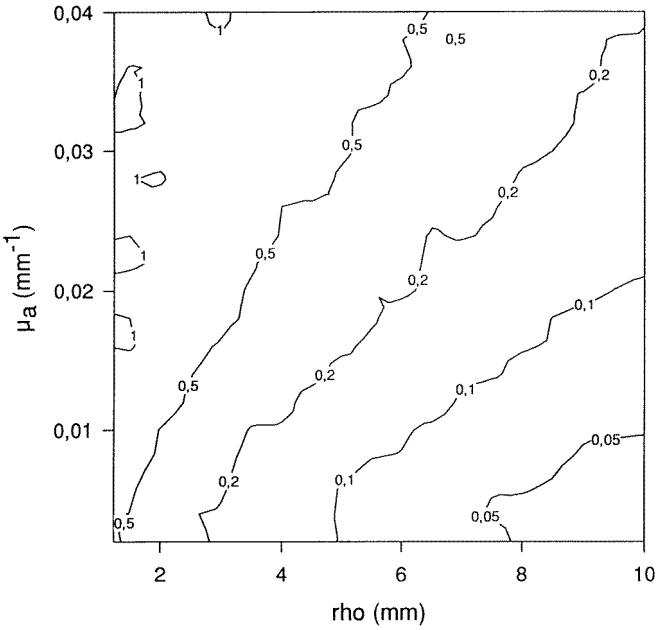

Figure 5. σ_a versus μ_a and ρ for $\mu_s' = 1$ mm^{-1} and $f = 200$ MHz determined from phase and modulation measured at a single distance.

(the reduced scattering coefficient) is determined. (In some cases the nonlinear regression did not converge if the added error was large. In this case these results were disregarded and the calculations were continued until 200 nonlinear regressions were successful.) This process was repeated for the parameter range indicated in the introduction. Contour lines of σ_a and σ_s were plotted versus the absorption coefficient and the distance between source and detector. Phase/steady-state reflectance as well as phase/modulation data were considered for measurements at one distance ρ and at two distances. For data measured at two distances, the first distance ρ_2 was half of the second distance ρ. In the following we concentrate on the determination of the absorption coefficient but the reduced scattering coefficient is also considered.

Figure 5 shows contour lines of constant σ_a for $\mu_s' = 1$ mm^{-1} and $f = 200$ MHz determined from phase and modulation data measured at one distance for 0.002 mm$^{-1} < \mu_a < 0.04$ mm^{-1} and 1.25 mm $< \rho < 10$ mm. The relative error in μ_a increases if the distance is decreased because the phase and the demodulation decrease. For the same reason σ_a also increases if μ_a is increased. The errors in the reduced scattering coefficient (figure not shown) are in this case similar to those of the absorption coefficient. If σ_a is calculated under the same conditions as above but based on phase and modulation data at two distances, the greater distance being equal to the distance of the single detector in the case of the measurements at one distance, then the relative errors in μ_a and μ_s' are larger. This is because the phase difference and the demodulation for the data measured at two distances are smaller resulting in a greater relative error.

Figure 6 (figure 7) shows the contour lines of σ_a (σ_s) for $\mu_s' = 1$ mm^{-1} and $f = 200$ MHz determined from phase difference and steady-state reflectance ratio data between two distances for the same range of μ_a and ρ values as in figure 5. As in figure 5, the error in μ_a increases if ρ decreases but the error does not depend significantly on μ_a for $\mu_a > 0.01$ mm^{-1}. This is probably because the difference in steady-state reflectance at the two distances is smaller for smaller μ_a resulting in a greater relative error. This seems to compensate the μ_a dependence of the phase error explained above. The main feature, however, is that the errors are everywhere smaller than those in figure 5. The reason for this is that the measurement of the demodulation has higher relative uncertainty than the measurement of the steady-state reflectance under these conditions. The errors in the estimated reduced scattering coefficient are smaller than those in the absorption coefficient (see figure 7). This can be understood from the following argument. The steady-state reflectance does not depend strongly on the absorption coefficient for small distances (figure 2). Thus, the absorption coefficient is mainly determined from the phase data which have larger relative errors than the steady-state reflectance data.

We also investigated σ_a and σ_s for phase and steady-state reflectance measured at a single distance. These plots (not shown) show regions for certain ρ and μ_a values where σ_a or σ_s are very large or where the determination of the optical properties is not possible. This behaviour is caused by the ambiguity discussed in section 2.3. However, outside these regions, the errors are smaller than the errors associated with the phase and steady-state reflectance data at two distances. Because of the poor performance of the estimation based on phase and modulation and the ambiguity of the solution which uses the phase and steady-state reflectance at one distance, we concentrate in the following on the strategy employing the phase and steady-state reflectance data measured at two distances.

Figure 8 shows a contour plot for the same conditions as used for figure 6 except the reduced scattering coefficient has been reduced to $\mu_s' = 0.5$ mm^{-1}. This results in an increase of the error in the absorption coefficient, because decreasing μ_s' means that the phase is decreased and, thus, the relative error in the determination of the phase is increased

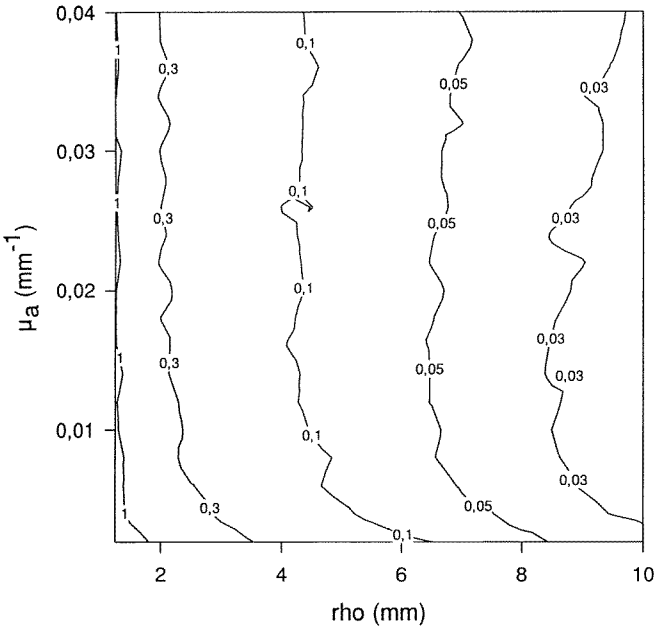

Figure 6. σ_a versus μ_a and ρ for $\mu_s' = 1$ mm^{-1} and $f = 200$ MHz determined from phase difference and steady-state reflectance ratio measured at two distances. The detectors are located at ρ and $\rho/2$.

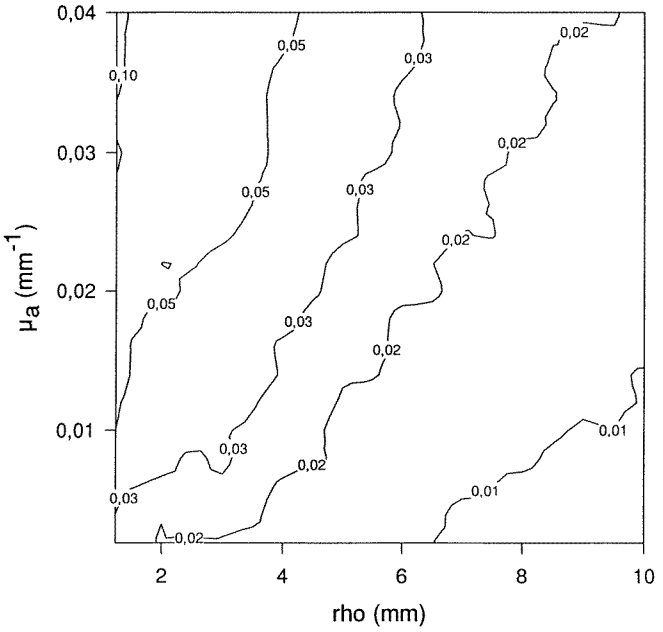

Figure 7. σ_s versus μ_a and ρ for $\mu_s' = 1$ mm^{-1} and $f = 200$ MHz determined from phase difference and steady-state reflectance ratio measured at two distances. The detectors are located at ρ and $\rho/2$.

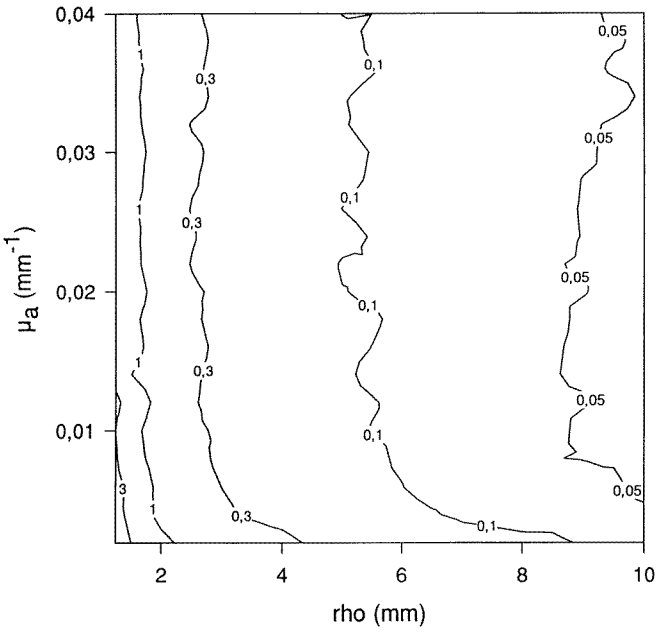

Figure 8. σ_a versus μ_a and ρ for $\mu_s' = 0.5$ mm^{-1} and $f = 200$ MHz determined from phase difference and steady-state reflectance ratio measured at two distances. The detectors are located at ρ and $\rho/2$.

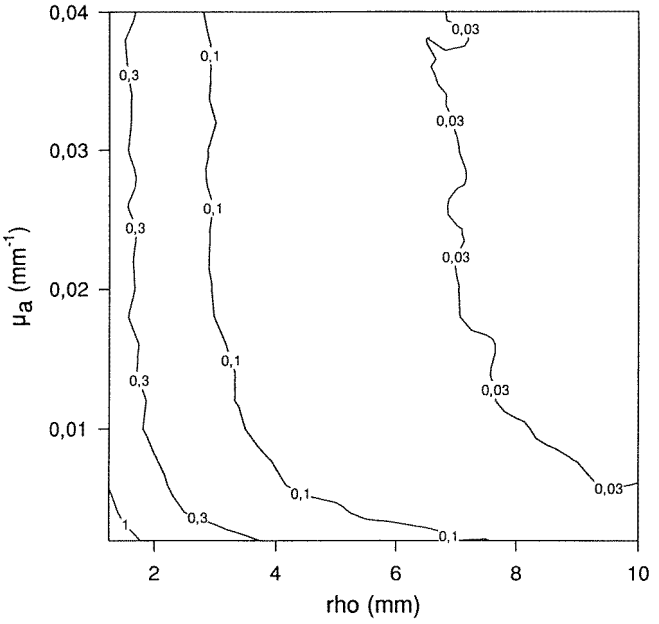

Figure 9. σ_a versus μ_a and ρ for $\mu_s' = 0.5$ mm^{-1} and $f = 500$ MHz determined from phase difference and steady-state reflectance ratio measured at two distances. The detectors are located at ρ and $\rho/2$.

(this is also the case for the steady-state reflectance). We note that the same arguments are also valid for the errors in the reduced scattering coefficient (data not shown).

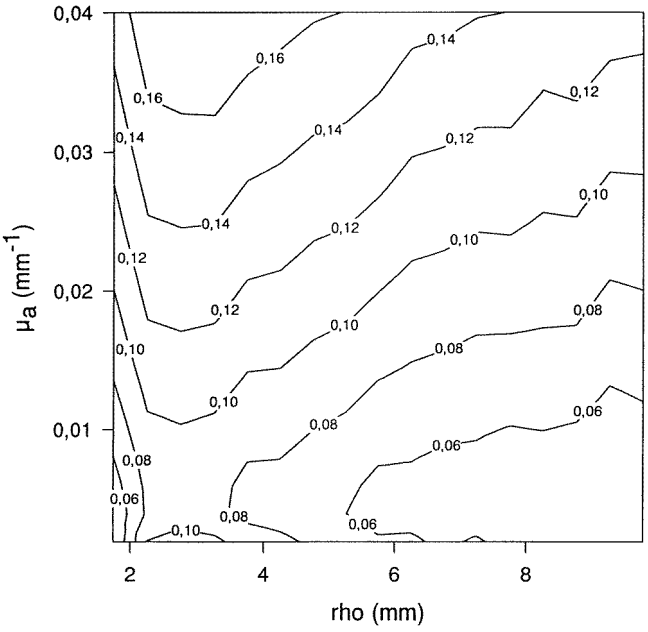

Figure 10. χ_a versus μ_a and ρ for $\mu_s' = 1$ mm^{-1} and $f = 195$ MHz determined from phase and modulation data at a single distance using equation (10).

In order to decrease the errors in the determination of μ_a and μ_s' the modulation frequency can be increased, because this increases the absolute phase difference between detectors and, thus, decreases the relative error in the phase. Figure 9 shows σ_a for the same parameters as in figure 8 but the frequency was changed from $f = 200$ MHz to $f = 500$ MHz. Figure 9 indicates the expected decrease of the errors. We note that although we assumed that the errors of the phase are the same for $f = 500$ MHz and $f = 200$ MHz it is in general more difficult to achieve the required phase accuracy at higher frequencies.

4. Errors caused by using diffusion theory

In this section we consider errors in μ_a and μ_s' caused by fitting solutions of the diffusion equation to Monte Carlo simulations which were generated as described in section 2.2. To be able to compare the errors caused from uncertainties due to the measuring apparatus with those due to the application of the diffusion equation we first present contour plots for the same conditions as the plots in section 3. (The modulation frequency is slightly different because of the sampling interval used in the Monte Carlo simulations.) For these calculations, equation (10) was applied as the solution of the diffusion equation; equations (5) and (9) are considered later.

The difference between the optical parameters obtained from nonlinear regression and the correct values divided by the correct values were calculated. In the following we term these relative errors in μ_a and μ_s', χ_a and χ_s respectively.

Figure 10 shows χ_a versus ρ and μ_a for a reduced scattering coefficient of $\mu_s' = 1\ \mathrm{mm}^{-1}$ and a frequency of 195 MHz. The phase and the modulation at a single distance were used to estimate μ_a and μ_s'. This figure corresponds to figure 5 of section 3. The errors shown in figure 10 are generally smaller than those in figure 5, especially at small distances. We note that the errors in reduced scattering coefficient (data not shown) are greater than in the absorption coefficient.

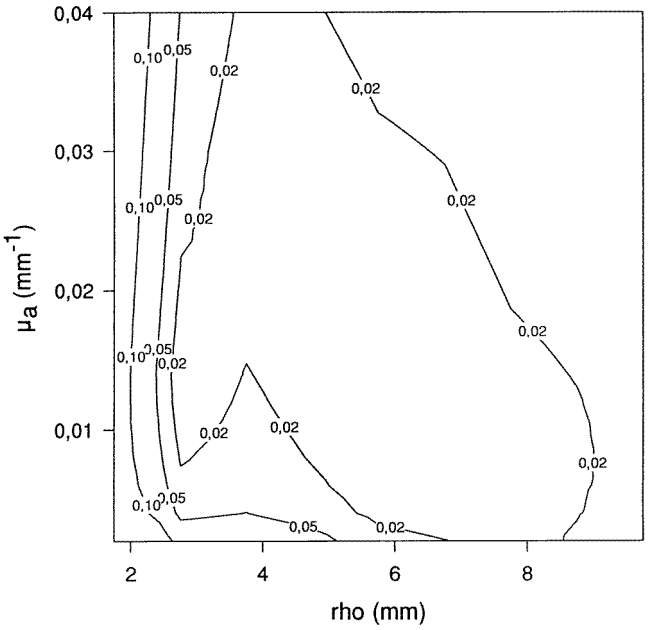

Figure 11. χ_a versus μ_a and ρ for $\mu_s' = 1\ \mathrm{mm}^{-1}$ and $f = 195$ MHz determined from phase difference and steady-state reflectance ratio data at two distances using equation (10). The detectors are located at ρ and $\rho/2$.

Figure 11 (figure 12) shows the contour lines of χ_a (χ_s) for $\mu_s' = 1\ \mathrm{mm}^{-1}$ and $f = 195$ MHz determined from phase and steady-state reflectance data measured at two distances corresponding to figure 6 (figure 7) in section 3. Whereas the errors in deriving μ_s' are comparable (figure 12 compared to figure 7), the errors in deriving μ_a are much smaller in figure 11 than in figure 6. This means that, for the derivation of the absorption coefficient, the error caused from the uncertainty in the measurement apparatus is more important than that caused from the diffusion approximation.

Figure 13 gives χ_a for the same data as above but μ_s' is changed to $0.5\ \mathrm{mm}^{-1}$. As expected, the errors increase if the reduced scattering coefficient is decreased. However, they are smaller than the errors caused from the uncertainties in measuring the phase and intensities (figure 8).

Figure 14 shows χ_a at 488 MHz for $\mu_s' = 0.5\ \mathrm{mm}^{-1}$. The errors are similar to the errors in figure 13. (In general, the errors in deriving μ_a and μ_s' caused by the diffusion approximation show either almost no dependence on the frequency or they increase if the frequency is increased.) Comparing figure 14 with figure 9 it can be seen that errors in deriving μ_a are similar. Thus, the approximations of the diffusion theory and the uncertainties of the experimental apparatus are equally important in this case.

In order to investigate the performance of equation (5) and equation (9) compared with

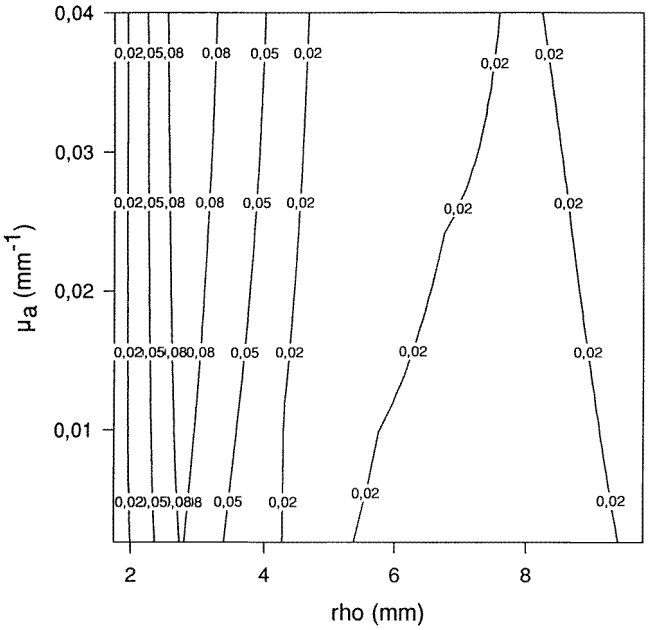

Figure 12. χ_s versus μ_a and ρ for $\mu_s' = 1$ mm^{-1} and $f = 195$ MHz determined from phase difference and steady-state reflectance ratio data at two distances using equation (10). The detectors are located at ρ and $\rho/2$.

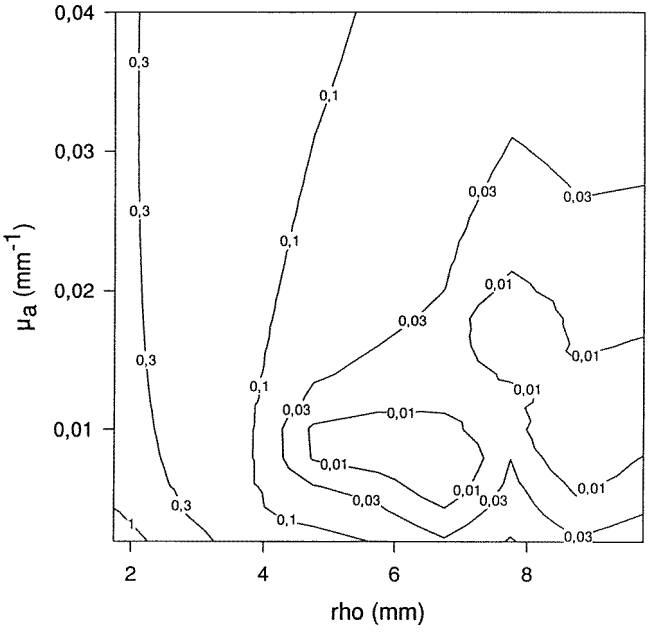

Figure 13. χ_a versus μ_a and ρ for $\mu_s' = 0.5$ mm^{-1} and $f = 195$ MHz determined from phase difference and steady-state reflectance ratio data at two distances using equation (10). The detectors are located at ρ and $\rho/2$.

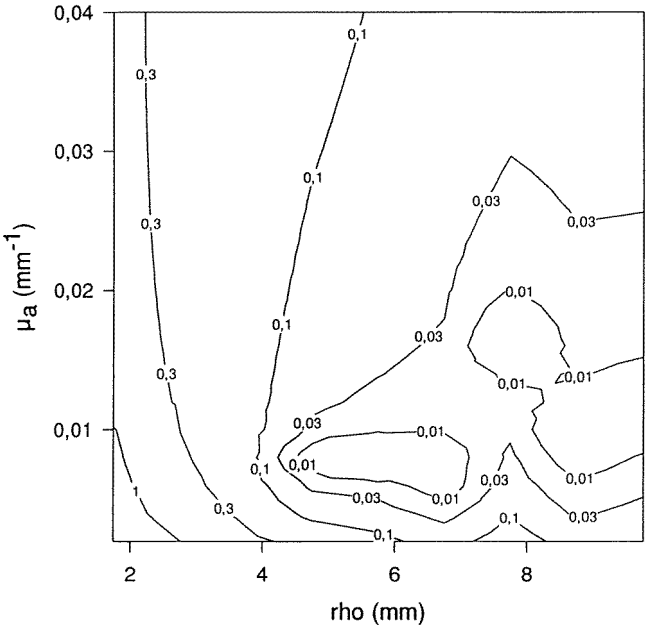

Figure 14. χ_a versus μ_a and ρ for $\mu_s' = 0.5$ mm^{-1} and $f = 488$ MHz determined from phase difference and steady-state reflectance ratio data at two distances using equation (10). The detectors are located at ρ and $\rho/2$.

equation (10), χ_a and χ_s were calculated using these equations to fit Monte Carlo simulations for the parameter range indicated in the introduction. Figures 15 and 16 show χ_a using equations (5) and (9) respectively for $\mu_s' = 1.0$ mm^{-1} and $f = 195$ MHz and phase and steady-state reflectance data measured at two distances. The performance of equation (5) is worse compared to that of equation (10) (see figure 11), whereas that of equation (9) is much worse. For equation (9) it is not possible to determine the optical coefficients for distances less than ≈ 4 mm, because the nonlinear regression does not converge. This behaviour, that equation (9) is considerably and equation (5) is, in general, slightly worse than equation (10) has been observed for the whole considered parameter range indicated in the introduction.

5. Discussion

We investigated the influence of typical experimental uncertainties and inaccuracy in the diffusion approximation on estimates of the optical properties of tissue based on frequency-domain reflectance measurements for a semi-infinite medium close to the source. It was shown that the measurement of the phase and steady-state reflectance at one distance does not always deliver a unique solution for the reduced scattering coefficient and the absorption coefficient. Thus, it must be carefully checked if this approach is feasible under the expected conditions.

Investigating the influence of the experimental uncertainties we found, in general, that the errors in determining μ_a and μ_s' are greater for frequency-domain data at two distances compared with data at one distance if the distance of the farther detector in the case of the 'two-detector' data equals the distance of the single detector in the case of the 'one-

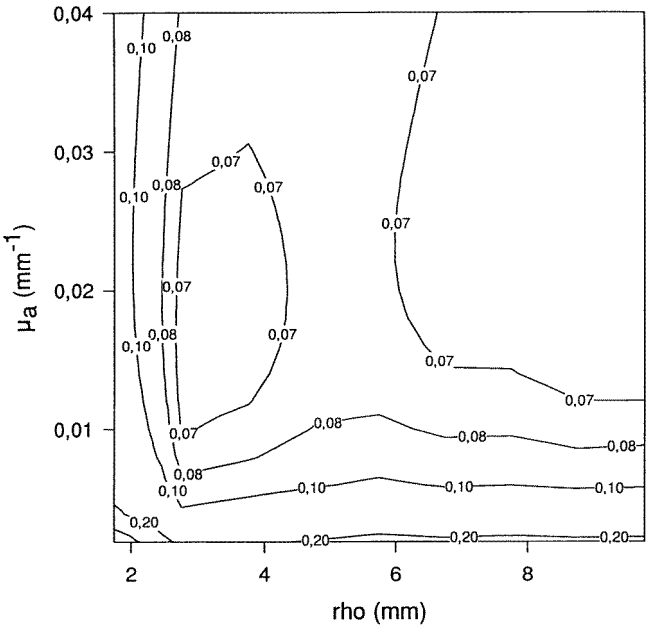

Figure 15. χ_a versus μ_a and ρ for $\mu_s' = 1$ mm^{-1} and $f = 195$ MHz determined from phase difference and steady-state reflectance ratio data at two distances using equation (5). The detectors are located at ρ and $\rho/2$.

detector' data. It was also shown that the errors are smaller if the phase and the steady-state reflectance are measured rather than the phase and modulation. Thus, in principle, the phase and steady-state reflectance data at one distance are least affected by the errors in the measuring apparatus. However, because the determination of the optical properties is not always unique in this case, we propose the measurement of the phase and steady-state reflectance at two distances as the best alternative. Measurements at one distance also present other difficulties: for example, calibration of the apparatus would require baseline measurements on a tissue-simulating phantom with accurately known optical properties. This procedure will result in additional errors that have not been considered in this study.

For the measurements using phase difference and steady-state reflectance ratio between two distances we found that the reduced scattering coefficient can be determined with errors smaller than 10% at distances as close as 2 mm for typical optical coefficients in the near-infrared and $f = 200$ MHz. The errors in determining the absorption coefficient are considerably higher. Roughly, the errors in μ_a exceed 10% for distances smaller than about 5 mm. It was shown that the errors can be reduced if the modulation frequency is increased.

Regarding the errors due to the application of the diffusion equation, it is favourable to make measurements at two distances, because the errors due to the poor performance of the diffusion approximation immediately at the source can be avoided. Whereas we found that the errors for the phase and modulation methods are similar to those for phase and steady-state reflectance, the errors attributable to different solutions of the diffusion equation vary considerably. The solution which uses the flux and the fluence terms (equation (10)) performs, in general, better than equation (5) and much better than equation (9).

In general, the errors in determining the absorption coefficient which are due to the diffusion approximation are smaller than those which result from experimental uncertainties

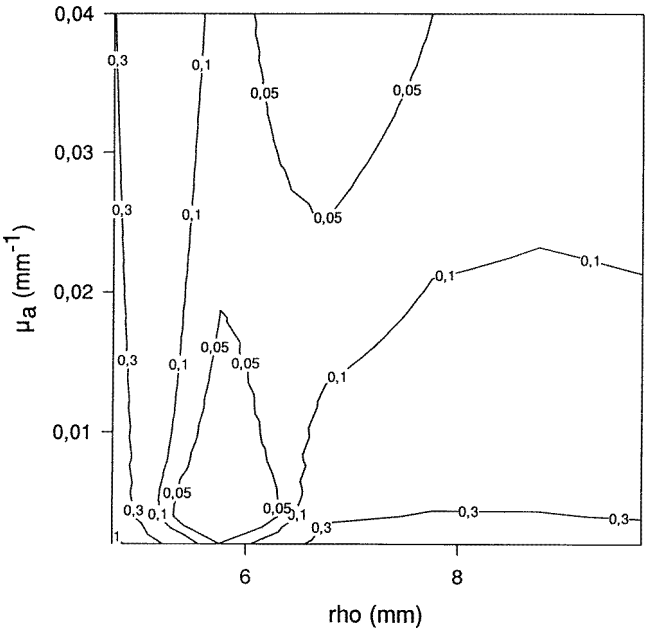

Figure 16. χ_a versus μ_a and ρ for $\mu_s' = 1$ mm^{-1} and $f = 200$ MHz determined from phase difference and steady-state reflectance ratio data at two distances using equation (9). The detectors are located at ρ and $\rho/2$.

if low modulation frequencies (200 MHz) and phase difference and steady-state reflectance ratio data at two distances are used.

The errors due to the application of the diffusion approximation can be avoided if Monte Carlo simulations are used as the theoretical description of light propagation in turbid media. Because the iterative use of Monte Carlo simulations for determination of the optical properties requires long computation time, we developed an approach which allows determination of the reduced scattering and absorption coefficients of semi-infinite turbid media from a single Monte Carlo simulation (Kienle and Patterson 1996). We showed for time-domain data that this is possible using scaling techniques. This 'Mono Monte Carlo' approach can also be used in the frequency domain if the time-domain data are Fourier transformed at every iteration. We investigated the Mono Monte Carlo technique in the frequency domain for the parameters used above by using this method to fit the results of the independent Monte Carlo simulations described in section 2.3. No experimental errors were added. We found that the errors in determining μ_s' and μ_a were about 1% for $\rho\mu_s' \approx 10$, about 2% for $\rho\mu_s' \approx 5$ and about 5% for $\rho\mu_s' \approx 2.5$. These relatively small errors result from interpolation errors in the scaling procedure due to the finite spatial resolution of the Monte Carlo simulations and can be reduced using a finer grid of stored data versus distance.

Acknowledgments

This work was supported by the National Institutes of Health grant PO1-CA43892. Alwin Kienle is grateful for a post-doctoral scholarship from the German Research Society (Deutsche Forschungsgemeinschaft).

References

Arridge S R, Cope M and Delpy D T 1992 The theoretical basis for the determination of optical pathlengths in tissue: temporal and frequency analysis *Phys. Med. Biol.* **37** 1531–60

Bevington P R 1983 *Data Reduction and Error Analysis for the Physical Sciences* (New York: McGraw-Hill) ch 11

Bocher T, Beuthan J, Minet O, Naber R and Müller G 1995 Frequency domain technique for a 2-dimensional mapping of optical tissue properties *SPIE Proc.* **2626** 54–64

Bolin F P, Preuss L E, Taylor R C and Ference R J 1989 Refractive index of some mammalian tissue using a fiber optic cladding method *Appl. Opt.* **28** 2297–303

Bolt R A and ten Bosch J J 1994 On the determination of optical parameters for turbid materials *Waves Random Media* **4** 233–42

Cope M and Delpy D T 1988 System for long term measurement for cerebral blood and tissue oxygenation on newborn infants by near infrared transillumination *Med. Biol. Eng. Comput.* **26** 289–94

Fantini S, Franceschini M A, Fishkin S, Barbieri B and Gratton E 1994 Quantitative determination of the absorption spectra of chromophores in strongly scattering media: a light emitting-diode based technique *Appl. Opt.* **33** 5204–13

Farrell T J, Patterson M S and Wilson B C 1992 A diffusion theory model of spatially-resolved, steady-state diffuse reflectance for the noninvasive determination of tissue optical properties *in vivo Med. Phys.* **19** 879–88

Graaff R, Koelink M H, de Mul F F M, Zijlstr W G, Dassel A C M and Aarnoudse J G 1993 Condensed Monte Carlo simulations for the description of light transport *Appl. Opt.* **32** 426–34

Haskell R C, Svaasand L O, Tsay T T, Feng T C, McAdams M and Tromberg B J 1994 Boundary conditions for the diffusion equation in radiative transfer *J. Opt. Soc. Am.* **11** 2727–41

Henyey L G and Greenstein J L 1941 Diffuse radiation in galaxy *Astrophys. J.* **93** 70–83

Hielscher A H, Jacques S L, Wang L and Tittel F K 1995 The influence of boundary conditions on the accuracy of diffusion theory in time-resolved reflectance spectroscopy of biological tissue *Phys. Med. Biol.* **40** 1957–75

Ishimaru A 1978 *Wave Propagation and Scattering in Random Media* (New York: Academic) ch 7 and 9

Kienle A, Lilge L, Patterson M S, Hibst R, Steiner R and Wilson B C 1996 Spatially-resolved absolute diffuse reflectance measurements for non-invasive determination of the optical scattering and absorption coefficients of biological tissue *Appl. Opt.* **35** 2304–14

Kienle A and Patterson M S 1996 Determination of the optical properties of turbid media from a single Monte Carlo simulation *Phys. Med. Biol.* **41** 2221–7

——1997 Improved solutions of the steady-state and time-resolved diffusion equations for reflectance from a semi-infinite turbid medium *J. Opt. Soc. Am.* A **14** 246–54

Moulton J D 1990 Diffusion modelling of picosecond laser pulse propagation of turbid media *Master's Dissertation* McMaster University, Hamilton, Ontario

Pogue B W and Patterson M S 1994 Frequency-domain optical absorption spectroscopy of finite tissue volumes using diffusion theory *Phys. Med. Biol.* **39** 1157–80

——1996 Error assessment of a wavelength tunable frequency domain system for noninvasive tissue spectroscopy *J. Biomed. Opt.* **1** 311–23

Press W H, Flannery B P, Teukolsky S A and Vetterling W T 1990 *Numerical Recipies in Pascal* (Cambridge: Cambridge University Press)

Tearney G J, Brezinski M E, Southern J F, Bouma B E, Hee M R and Fujimoto J G 1995 Determination of the refractive index of highly scattering human tissue by optical coherence tomography *Opt. Lett.* **20** 2258–60

Wang L, Jacques S L and Zheng L 1995 MCML–Monte Carlo modelling of light transport in multi-layered tissues *Comput. Methods Programs Biomed.* **47** 131–46

Wilson B C and Adam G 1983 A Monte Carlo model for the absorption and flux distribution of light in tissue *Med. Phys.* **10** 824–30